Article

Not peer-reviewed version

Ru-Based NSAIDs Anticancer Potential Therapeutics

Silvia Bordoni *, Magda Monari, Carla Boga *, Federico Moro, Giacomo Drius

Posted Date: 19 January 2026

doi: 10.20944/preprints202601.1312.v1

Keywords: metallo-prodrugs; ruthenium; SCXRD; cancer

 doi:10.20944/preprints202601.1312.v1

Article

Ru-Based NSAIDs Anticancer Potential Therapeutics

Silvia Bordoni [1,*], Magda Monari [2], Carla Boga [1,*], Federico Moro [1] and Giacomo Drius [1]

[1] Department of Industrial Chemistry 'Toso Montanari', Alma Mater Studiorum, Università di Bologna, Via Piero Gobetti, 85, 40129, Bologna, Italy

[2] Department of Chemistry 'Giacomo Ciamician', Alma Mater Studiorum, Università di Bologna, Via Piero Gobetti, 85, 40129, Bologna, Italy

* Correspondence: silvia.bordoni@unibo.it (S.B.); carla.boga@unibo.it (C.B.)

Abstract

The use of metal-based species bearing existing pharmaceuticals as ligands, often resulting in enhanced bioactivity, represents an attractive strategy for the development of novel therapeutic formulations. In the context, five well-known non-steroidal anti-inflammatory drugs (NSAIDs) were employed to substitute both PPh_3 and hydride ligands in $[Ru(H)_2(CO)(PPh_3)_3]$ (**1**), selectively affording, via molecular hydrogen release, neutral κ^2-(O,O)-chelate complexes in satisfactory yields. Among the obtained species, two complexes coordinating diclofenac (**4**) and aspirin (**5**) were further investigated by single-crystal X-ray diffraction (SCXRD). Preliminary biological studies on the ruthenium-salicylic acid species **2** showed promising antiproliferative activity against HeLa cancer cells, consistent with the fact that NSAID–ruthenium(II) complexes represent a well-established research area for the development of novel anticancer metallotherapeutics.

Keywords: metallo-prodrugs; ruthenium; SCXRD; cancer

1. Introduction

The increasing societal impact of cancer prompted the scientific community to seek novel chemotherapeutic agents with reduced side effects. The search for novel and effective anticancer agents has fuelled a growing interest in the development of transition metal complexes encompassing biologically relevant molecules. Metal-based species containing versatile ruthenium coordinating multi-functionalized ligands undoubtedly occupy a prominent position in this field [1–6]. Non-steroidal anti-inflammatory drugs (NSAIDs) constitute a well-known wide class of medications to treat pains and inflammations, which exhibit similar pharmacological properties, mechanisms of action and side effects [7]. The compounds possess a variety of biological activities due to their ability to bind plasma proteins, primarily ascribed to amphiphilic properties. Their structure includes hydrophilic groups such as carboxyl- or enol- functions beside lipophilic groups as aromatic rings or halide units [8,9].

Cyclooxygenase enzymes are known to play a crucial role in inflammation and carcinogenesis by catalysing the conversion of arachidonic acid into prostaglandins [10]. NSAIDs have demonstrated to be notably inclined to prevent different kinds of cancers, including breast, lung, and colorectal [11], through a non-selective inhibition of cyclooxygenase-1 (COX-1), cyclooxygenase-2 (COX-2), and lipoxygenase metabolism (LOX), which play a significant role in angiogenesis by promoting migration of the endothelial cells [12].

In the last decades, multiple studies demonstrated the existence of a strong correlation between inflammation and cancer development. Combinatory action, ascribable to the synergistic therapeutic effects, expressed by the anti-inflammatory results with Ru-based potential anticancer activities have been recently demonstrated to be more than a speculation [13,14]. NSAID-Ruthenium (II) complexes represent a promising area of research in the development of novel anticancer treatments that leverage the combined benefits of anti-inflammatory and anticancer effects. In fact, dual functionality

 doi:10.20944/preprints202601.1312.v1

offers an alternative approach, targeting both inflammation and neoplastic growth, and in certain cases, improving efficacy and selectivity, compared to fragments alone. Recently, the group of Martling reported a remarkable result, relating low dose of aspirin to control localized colorectal cancer [15]. These types of organo-inorganic systems are reported to exhibit advantages in enhancing therapeutic value by the joined ability of anti-inflammatory features with Ru-anticancer potential [16].

The presence of the metal is crucial in facilitating interactions with biomolecules by inducing structural alterations [17–21] thanks to more robust frameworks and the aptitude to interfere with biological paths, which can lead to cell death by apoptosis or anti-angiogenic processes. The biological responses are indeed attributable to the synergistic effects of the metal ion core interacting with NSAID pharmacophores [10]. Several studies reported the success of [Ru(η^6-p-cymene)(NSAID)Cl], coordinating ibuprofen, aspirin, naproxen and diclofenac as κ^2-(O,O)-chelate ligands (Figure 1) [20,22]. The obtained complexes demonstrated interesting antiproliferative activity against different cancer cell lines.

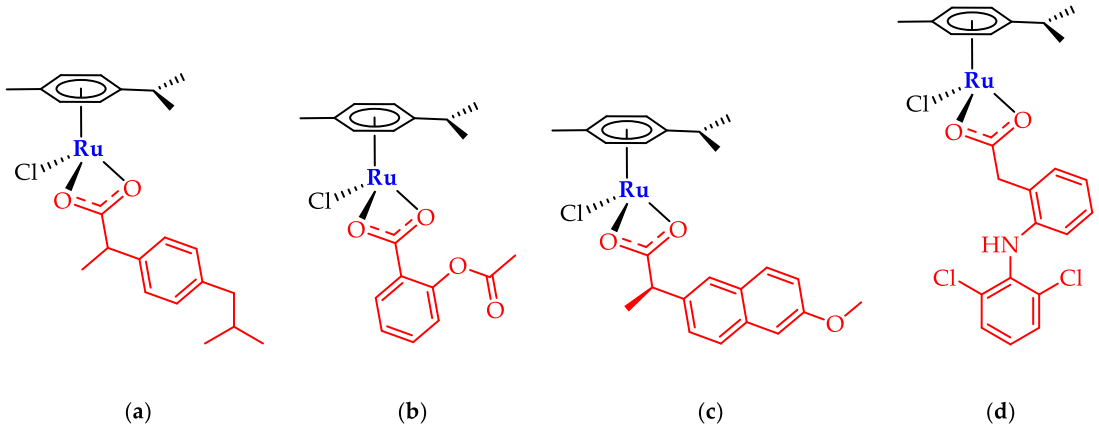

Figure 1. Piano stool [Ru(η^6-p-cymene)(NSAID)Cl] complexes with (**a**) ibuprofen, (**b**) aspirin, (**c**) naproxen and (**d**) diclofenac, Mandal (**2018**).

The above class of Ru-complexes demonstrated a promising antiproliferative activity against various cancer cell lines as cervical (HeLa), breast (MCF-7), lung (A549) tumors, with growth-inhibition values comparable to the current most efficient antineoplastic drugs [22]. Alternative structures as analogous Ru-phosphine complexes have been scarcely explored, albeit they present IC_{50} values lower than cisplatin on the tested cell lines. In particular, on the MCF-7 breast cancer cell line, [Ru(dppe)$_2$(A)] (Figure 2a) shows IC_{50} value of 3.46 ± 0.04 μM, compared to 8.91 ± 2.59 μM for cisplatin; while [Ru(bipy)(dppp)(A)] (Figure 2b) exhibits IC_{50} value of 0.66 ± 0.04 μM, remarkedly lower than cisplatin (11.80 ± 0.80 μM) on A2780 ovarian cell line [23–26].

Further, the cyclometalated Ru-complex [Ru(CCC-Nap)(Ibu)(PTA)] (Figure 2c), concomitantly incorporating ibuprofen and naproxen-derived ligand, displays a significant cancer cells cytotoxicity [27–29]. The structural similarity with the *trans*-phosphines complexes described by Correa [Ru(PPh$_3$)$_2$(Th)(bipy)]PF$_6$, in which Th indicates thiourea derivatives [30], and Baratta groups [Ru(OAc)(acac)(PPh$_3$)$_2$] [31], prompted to assume analogous amphiphilic properties for our class of metal systems.

 doi:10.20944/preprints202601.1312.v1

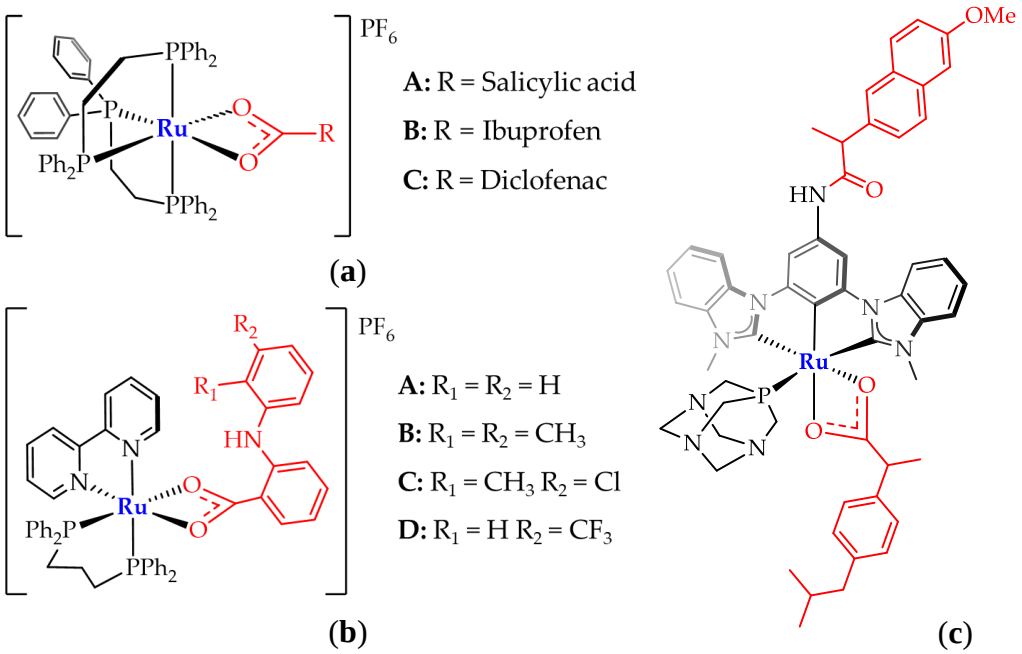

Figure 2. Ruthenium-NSAIDs complexes encompassing phosphine ligands. (**a**) Graminha (**2022**) and Von Poelhsitz (**2015**), (**b**) Correa (**2025**), (**c**) Tabrizi (**2018**).

2. Results and Discussion

Complexes of general formula [RuH(CO)(PPh_3)$_2$(NSAID)] were yielded in 49-79% range by reaction of the parent (**1**) [Ru(H)$_2$(CO)(PPh_3)$_3$] with slight excess of NSAID, to obtaining the expected Ru(II)-NSAIDs complexes as unique species by selective H_2 release and elimination of a PPh_3 ligand. All the synthesized complexes were treated by Et_2O extractions and recrystallized. Their proposed structures were supported by analytical and spectroscopic data through ESI-MS, FTIR, ^{1}H, ^{31}P{^{1}H}, ^{13}C{^{1}H} NMR and UV-Vis spectra (Scheme 1).

2.1. Infrared Spectroscopy

IR spectra analyses are in agreement with the proposed structures. The IR spectra of **3**-**6** evidence asymmetric carboxy-absorptions in 1634-1521 cm^{-1} interval, close to the lower frequency set of bands (1526-1455 cm^{-1}) attributable to the symmetric stretching. These signals are diagnostic for a dihapto coordination mode, that allows the formation of 4-membered metallacycles. Intermolecular H-binding network can be invoked, promoted by aryl-substituent lone pairs as hydroxyl or methoxy- for the salicylate class of ligands as well as chloride for coordinated diclofenac. In the case of complex **2** (Scheme 1), the coordination of the salicylate ligand is supported by the occurrence of OH. Useful comparisons are provided in Table 1.

Table 1. Selected bands observed in FTIR spectra of complexes **2-6**. Wavenumbers are reported in cm^{-1}.

Entry	Name	Formula	ν (CH)ar	ν (Ru-H)	ν (C≡O)	ν (COO)
2	Ru-Salicylic acid	[RuH(CO)(PPh_3)$_2$(Sal)]	3053, vw	2001, w	1927, s	*asym* 1533, w; *sym* 1332, w
3	Ru-Naproxen	[RuH(CO)(PPh_3)$_2$(Nap)]	3055, w	Overlapped	1923, s	*asym* 1634, w; *sym* 1526, m
4	Ru-Diclofenac	[RuH(CO)(PPh_3)$_2$(Dicl)]	3053, vw	2078, w	1915, s	*asym* 1557, m; *sym* 1455, m
5	Ru-Acetylsalicylic acid	[RuH(CO)(PPh_3)$_2$(MeOSal)]	3056, vw	2011, w	1909, s	*asym* 1571, w; *sym* 1465, m
6	Ru-Ibuprofen	[RuH(CO)(PPh_3)$_2$(Ibu)]	3056, w	1995, w	1924, s	*asym* 1521, m; *sym* 1458, m

 doi:10.20944/preprints202601.1312.v1

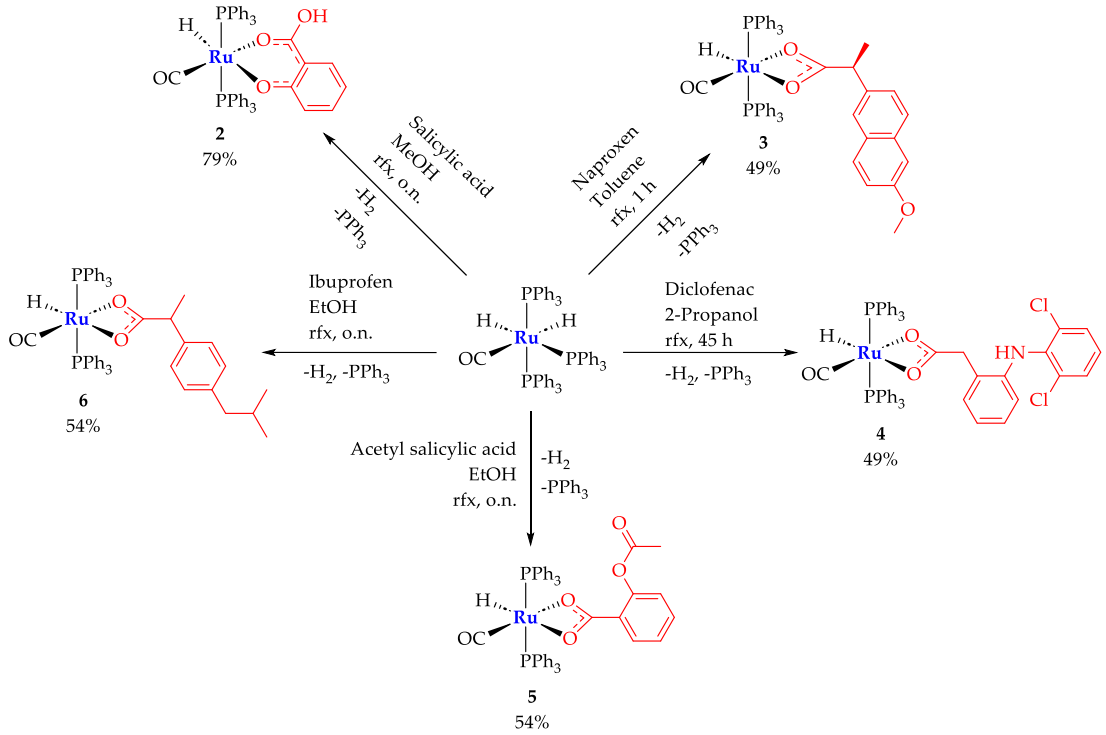

Scheme 1. Synthetic pathways and percentage yields for complexes **2**-**6**. All the products share the general formula [RuH(CO)(PPh_3)$_2$(NSAID)].

2.2. NMR Spectra of the Prepared Complexes

^{1}H, ^{31}P{^{1}H}, ^{13}C{^{1}H} and bidimensional COSY, HSQC and HMBC NMR spectra support the predicted molecular structure for the complexes **2**-**6**. Multiplets in the range of 7.64-7.14 ppm assess the presence of two triphenylphosphine ligands. In the precursor spectrum, two ^{1}H NMR signals are observed at -6.50 and -8.30 ppm, respectively. These are attributed to the highly shifted hydride ligands, whereas single hydride triplets are observed in the range -16.33 / -16.91 ppm in the spectra relative to complexes **2**-**6**, due to the coupling with the equivalent trans PPh_3, confirmed by the ^{31}P{^{1}H} NMR resonances in 43.09-44.60 ppm interval. The ^{13}C NMR spectra of **2**-**6** display a downfield triplet at about 205 ppm, assigned to Ru-CO, while the carboxylic carbon atoms singlets fall in the range 186.05-178.53 ppm (Table 2).

Table 2. Color, yield (%) and spectroscopical data of **2**-**6**. Chemical shifts are reported in ppm, UV-Vis absorptions in nm.

Entry	Name	Color	Yield	NMR			UV-Vis
				^{1}H - RuH	^{31}P{^{1}H} – PPh_3	^{13}C{^{1}H} – Ru(CO)	λ_{max}
2	Ru-Salicylic acid	Grey	79	-16.91	43.09	205.09	261
3	Ru-Naproxen	Red	49	-16.45	43.29	205.54	260
4	Ru-Diclofenac	Grey	49	-16.62	44.55	205.36	275
5	Ru-Acetylsalicylic acid	Grey	54	-16.32	44.58	205.48	274
6	Ru-Ibuprofen	White	53	-16.44	43.30	205.59	259

2.3. ESI-MS and UV Spectra

Mass Spectrometry provides fundamental information regarding the structure of complexes in solution. In the ESI-MS spectra of complexes **2** to **6**, acquired in MeCN, the most relevant peak is the one relative to [M – H]$^+$ composition. Other common fragments detected are: [M – H + MeCN]$^+$, [M – L + 2 MeCN]$^+$, [M – L + MeCN]$^+$ and [M – L]$^+$ (where L is the coordinated NSAID ligand). The latter appears as a high-intensity peak and it is related to the loss of O-donor ligands, confirming major

 doi:10.20944/preprints202601.1312.v1

metal affinity towards softer carbonyl and triphenylphosphine ligands. Isotopic peak patterns are all in good agreement with the simulated spectra.

The UV-Vis spectra of the complexes have been acquired in DMSO solution. A band in the range 259-275 nm has been observed in the analyzed species (Table 2) and attributed to intra-ligand charge transfer transition (ILCT). All recorded spectra are shown in supplementary information (Figures S7, S16, S24, S32, S40 Supplementary Material).

2.4. Description of the X-Ray Crystal Structures of 4 and 5

X-ray-quality crystals of **4** and **5** were grown by double-layer crystallization techniques (DCM-hexane = 1:10), and their structure was determined using SCXRD. In both structures, the ruthenium atom adopts a distorted octahedral geometry in which the PPh_3 ligands are in a mutual *trans*-position (Figures 1A and 1B) and one hydride, one carbonyl and one carboxylate ligands occupy equatorial coordination sites. The molecular structure of **4** shows an asymmetric chelate coordination of the carboxyl group of the diclofenac ligand [Ru-O1 2.183(2), Ru-O2 2.310(2) Å, respectively]. This is presumably due to the presence of the very bulky substituent (2,6-dichlorophenylamine) in the *ortho*-position of the benzyl ring, which is on the same side as O2. In addition, the conformation of the coordinated diclofenac ligand shows some differences from that found in the crystal structure of the diclofenac acid [32] being the dihedral angle between the least-squares planes of the two aromatic rings wider in the latter. Another significant effect attributable to steric crowdedness is the deviation from linearity of the P-Ru-P angle [171.94(3)°], which relieves the steric strain between the phenyl groups of the axial phosphines and the bulky diclofenac ligand. The two Ru-P distances are almost identical [Ru-P 2.3455(8) and 2.3458(9) Å]. Intramolecular hydrogen bonds in the diclofenac ligand also play an important role: in fact, the carboxylic oxygen O2 is involved in both classical [NH…O2] and non-classical hydrogen bonds [C23H23…O2 and C45H45…O2] with one phenyl ring from the two PPh_3 ligands, the most significant being the NH…O2 interaction [N1…O2 2.904(4) Å and N1-H1N…O2 150°]. In the crystal packing intermolecular H bonds are established through one of the two chlorine atoms (Cl2) and one H atom of the methylene moiety of the diclofenac belonging to adjacent molecules thus forming dimeric units (Figure S41). Furthermore, an important role is played by π-π interactions between two 2,6-dichlorophenyl rings [centroid-centroid distance 3.555 Å] of neighboring molecules generating dimers (Figure S41) different from the former ones generated by H bonds. To the best of our knowledge, very few ruthenium complexes bearing the diclofenac ligand coordinated in a chelate fashion have been crystallographically investigated [33].

In the crystal structure of **5** the Ru atom, the hydride, the CO, and most of the chelating acetylsalicylate ligand lie on a crystallographically imposed symmetry plane. This symmetry is broken by the carbonyl [C8 and O4] of the acetylsalicylate AcO group that is disordered over two positions below and above the aromatic ring plane with half occupancy. Also, in complex **5** the two Ru-O distances are significantly different [Ru-O1 2.318(5) and Ru-O2 2.165(5) Å], while the Ru-P distance [2.353(1) Å] is almost identical to those reported for **4.** The asymmetry in the carboxylate coordination is likely caused by steric hindrance, as the weaker Ru-O interaction involves O1, which is located in *ortho* position and on the same side as the bulky AcO- substituent. In the crystal packing of **5** in addition to intramolecular H bonds non classical intermolecular H bonds [C24-H24…O1, C6-H6…O2] are at work (Figure S42).

 doi:10.20944/preprints202601.1312.v1

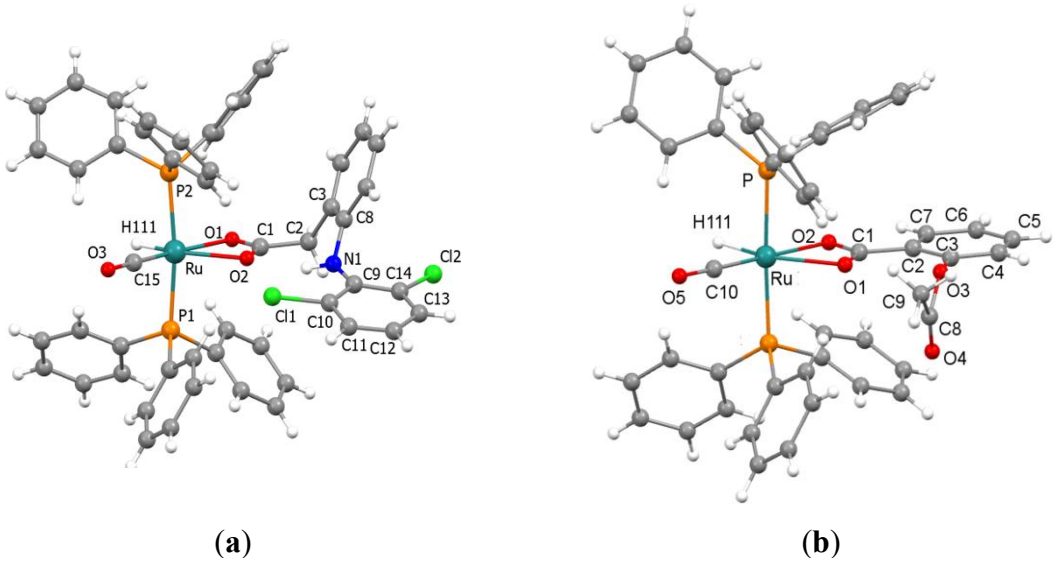

(**a**) (**b**)

Figure 1. Single crystal structures of complexes **4** (**a**) and **5** (**b**).

2.5. Stability in Aqueous Solution of **2**

A preliminary evaluation of the antiproliferative properties shown by complex **2** was performed using MTT assay. Prior to that, the stability in solution was evaluated by recording UV-Vis spectra in phosphate buffer solution (PBS-5% DMSO, pH 7.4) over a period of 48 hours. The spectra showed no wavelength shifts, indicating preserved structural integrity throughout the experiment duration (Figure S8, Supplementary Material).

2.6. Antiproliferative Activity of **2** *and* **6**

The anti-cancer ability of the ruthenium complexes **2** and **6** was evaluated using an MTT proliferation assay for HeLa cells. Dose-response graphs were constructed to determine the IC_{50} concentrations of various treatments and the results are shown in Figure 4 (A, B). Complex **6** shows no toxic activity at any of the concentrations tested, thus confirming that cytotoxicity is heavily dependent on the coordinated NSAID. In contrast, complex **2** shows an IC_{50} of 74.96 ± 0.82 μM. Interestingly, compound **2** shows an antiproliferative effect already at a concentration of 20 μM, reducing cell growth by 18.83 ± 5.75%. The in vitro antiproliferative properties of **2** are in line with other NSAIDs-ruthenium reported complexes [19,33].

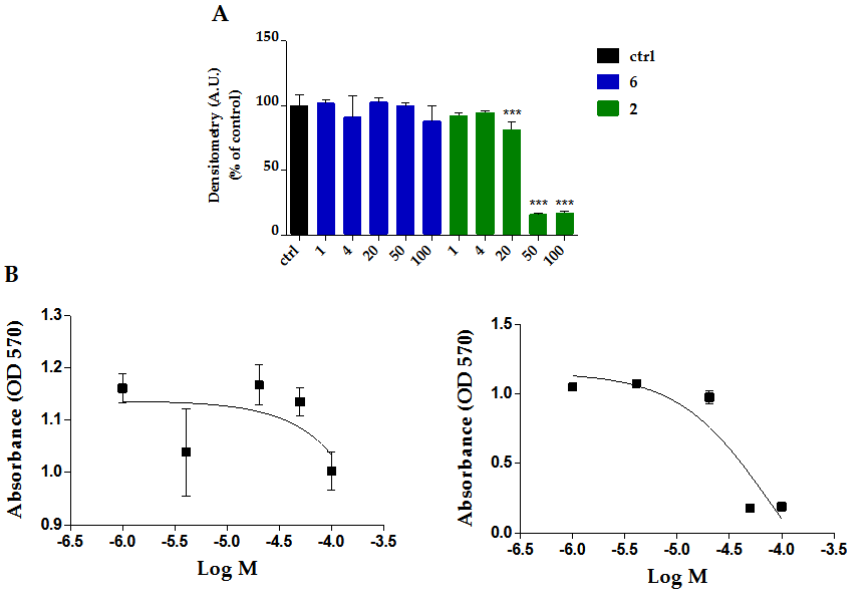

 doi:10.20944/preprints202601.1312.v1

Figure 2. Viability of HeLa cells in the presence of different concentrations of the compounds. A) The cells were treated for 24 hours with a concentration range of (1-100 μM) with compounds **2** or **6** dissolved in DMSO. Data are reported as the percentages of viable cells ± SDs in comparison to controls; n = 3. Cell viability was determined by the MTT assay, as described in the Material and Methods section. B) Dose response curves of HeLa cell viability upon treatment with different concentrations of (left) **6**, and (right) **2.**

In all cases, the NSAID ligands are coordinating via oxygen atoms of the carboxylate groups, except for salicylate in complex **2**, which anchored the carbonyl unit together with the phenolate group. Despite the difference shown in the coordinating fashion mode, remarkable bio-activity may suggest that pharmacokinetic paths could be similar to those evidenced by the analogous buffered aspirin derivative [34].

3. Materials and Methods

3.1. General

All the Ru-hydride adducts with NSAIDs have been obtained with the analogous procedure by optimizing the syntheses trough solvent's nature selection, so that the obtained adduct are insoluble. This triggers an almost complete selective precipitation, avoiding undesirable side/subsequent/co-reaction paths. Specific syntheses are listed below.

*3.2. Synthesis of Ru-Salicylic Acid Complex **2***

A small excess of salicylic acid (37 mg, 0.268 mmol) and $[Ru(H)_2(CO)(PPh_3)_3]$ **1** (220 mg, 0.240 mmol) were dissolved in methanol (15 mL) and refluxed overnight. By cooling down to room temperature a grey powder precipitate occurred. The solid was then filtered and washed with methanol (3 mL aliquots for 3 times), then dried under vacuum.

Yield: 79%. ATR-FTIR (ν, cm^{-1}): 3053 (aromatic CH), 2001 (RuH), 1927 (C≡O), 1625 (COOH), 1598 (C=C-C), 1464 (C=C-C), 1432 (CH, PPh_3), 1254 (C-O), 1095 (PPh). ^1H NMR (400 MHz, $CDCl_3$) (δ, ppm) 10.59 (1H, COOH, s), 7.53-7.30 (30H, PPh_3, m), 7.05 (1H, C-H, m), 7.03 (1H, C-H, m), 6.53 (1H, C-H, dd), 6.45 (1H, C-H, dt), -16.91 (1H, Ru-H, t, $^2J_{HP}$ = 20.04 Hz) , ^{13}C NMR (101 MHz, $CDCl_3$) (δ, ppm): 205.24 (Ru-C≡O, t), 178.53 (COOH), 159.81 (C-H), 133.08 (PPh_3), 133.05 (C-H), 129.97 (PPh_3), 129.79 (C-H), 128.25 (PPh_3), 117.52 (C-H), 116.03 (C-H), 115.91 (C-H). ^{31}P NMR (162 MHz, $CDCl_3$) (δ, ppm): 43.09 (2P, PPh_3). ESI-MS^+ (MeCN) (m/z): 791 $[M-H]^+$.

*3.3. Synthesis of Ru-Naproxen Complex **3***

Naproxen (63 mg, 0.272 mmol) and $[Ru(H)_2(CO)(PPh_3)_3]$ **1** (250 mg, 0.272 mmol) were dissolved in toluene (15 mL) and refluxed until the IR Ru-CO absorption of **1** at 1940 cm^{-1} disappeared. After 1 h the mixture was cooled down to room temperature and the solvent evaporated under vacuum. The powder was then dissolved in 1 mL of DCM and hexane (15 mL) was added to precipitate red powdered microcrystalline solid, which was then filtered, washed with hexane (3 times with 10 mL aliquots) and finally dried under vacuum.

Yield: 49%. ATR-FTIR (ν, cm^{-1}): 3055 (aromatic CH), 2929 (aliphatic CH), 1923 (C≡O), 1634 (asym. COO), 1606 (C=C-C), 1526 (asym. COO), 1455 (C=C-C), 1434 (CH, PPh_3), 1267 (C-O), 1095 (PPh). ^1H NMR (400 MHz, $CDCl_3$) (δ, ppm), 7.55-7.29 (30 H, PPh_3, m) 7.06-6.96 (5H, m), 6.60 (1H, CH, d), 3.90 (3H, OCH_3, s) 2.56 (1H, CH, q), 0.64 (3H, CH_3, d), -16.45 (1H, Ru-H, t, $^2J_{HP}$ = 21.45 Hz). ^{13}C NMR (101 MHz, $CDCl_3$) (δ, ppm): 205.54 (Ru-C≡O), 185.84 (COO), 157.19 (CH), 134.41 (PPh_3), 133.89 (CH), 132.20 (PPh_3), 129.79 (PPh_3), 128.72 (CH), 128.59 (CH), 128.15 (PPh_3), 127.53 (CH), 127.22 (CH), 126.20 (CH), 118.15 (CH), 105.61 (CH), 55.41 (CH), 47.85 (CH_3), 17.89 (OCH_3). ^{31}P NMR (162 MHz, $CDCl_3$) (δ, ppm): 43.29 (2P, PPh_3). ESI-MS^+ (MeCN) (m/z): 883 $[M-H]^+$.

 doi:10.20944/preprints202601.1312.v1

3.4. Synthesis of Ru-Diclofenac Complex ***4***

A small excess of Diclofenac (107 mg, 0.361 mmol) and $[Ru(H)_2(CO)(PPh_3)_3]$ **1** (276 mg, 0.301 mmol) were dissolved in 2-propanol (40 mL) and refluxed for 45 h. A grey powder precipitated by cooling down to room temperature. The solid was then filtered, washed with 2-propanol (3 mL aliquots x 3 times) and dried under vacuum.

Yield: 49%. ATR-FTIR (ν, cm^{-1}): 3263 (NH), 3053 (aromatic CH), 2079 (RuH), 1915(C≡O), 1578 (C=C-C), 1557 (asym. COO), 1455 (sym. COO), 1431 (CH, PPh_3), 1093 (PPh). ^{1}H NMR (400 MHz, $CDCl_3$) (δ, ppm), 7.64 (1H, NH, s), 7.44-7.14 (30 H, PPh3, m), 7.35 (1H, C-H, d), 6.96 (1H, CH, t), 6.87 (1H, CH, t), 6.52 (1H, CH, d), 6.32 (1H, CH, d), 6.24 (1H, CH, d), 2.51 (2H, CH_2, s), -16.69 (1H, Ru-H, t, $^2J_{HP}$ = 20.3 Hz) ^{13}C NMR (101 MHz, $CDCl_3$) 205.41 (Ru-C≡O, t), 183.99 (COO), 142.83 (CH), 138.72 (CH), 134.34 (PPh_3), 133.33 (PPh_3), 130.46 (CH), 129.88 (PPh_3), 129.73 (CH), 128.90 (CH), 128.23 (PPh_3), 126.68 (CH), 125.09 (CH), 123.29 (CH), 120.97 (CH), 117.28 (CH), 41.57 (CH_2). ^{31}P NMR (162 MHz, $CDCl_3$) (δ, ppm): 44.60 (2P, PPh_3). ESI-MS$^+$ (MeCN) (m/z): 948 $[M-H]^+$.

3.5. Synthesis of Ru-Acetyl Salicylic Acid Complex ***5***

Acetyl salicylic acid (39 mg, 0.218 mmol) and $[Ru(H)_2(CO)(PPh_3)_3]$ **1** (220 mg, 0.218 mmol) were dissolved in ethanol (15 mL) and refluxed overnight. A grey powder precipitated after cooling down the mixture solution to room temperature. The obtained solid was then filtered, washed with ethanol (3 times with 3 mL aliquots) and dried under vacuum.

Yield: 54%. ATR-FTIR (ν, cm^{-1}): 3056 (aromatic CH), 2011 (RuH), 1909 (C≡O), 1761 ($COOCH_3$), 1587 (C=C-C), 1571 (asym. COO), 1465 (sym. COO), 1433 (CH, PPh_3), 1200 (C-O). ^{1}H NMR (400 MHz, $CDCl_3$) (δ, ppm) 7.54-7.30 (30 H, PPh_3), 7.16 (1 H, CH, dt), 7.05 (1 H, CH, dd), 6.84 (1H, CH, dt), 6.69 (1 H, CH, dd), 2.10 (3 H, CH_3, s), -16.32 (1 H, RuH, t, $^2J_{HP}$ = 20.34), ^{13}C NMR (101 MHz, $CDCl_3$) (δ, ppm): 205.64 (C≡O), 185.08 (COO), 175.02 (C(O)OCH_3), 169.55 (C-O), 149.82 (C), 134.79 (PPh_3), 133.50 (PPh_3), 131.62 (CH), 131.50 (CH), 129.78 (PPh_3), 129.15 (PPh_3), 124.57 (CH), 122.75 (CH), 21.29 (CH_3). ^{31}P NMR (162 MHz, $CDCl_3$) (δ, ppm): 44.58 (2P, PPh_3). ESI-MS$^+$ (MeCN) (m/z): 833 $[M-H]^+$.

3.6. Synthesis of Ru-Ibuprofen Complex ***6***

A small excess of ibuprofen (31 mg, 0.150 mmol) was dissolved in EtOH (40 mL) solution of $Ru(H)_2(CO)(PPh_3)_3$] **1** (113 mg, 0.123 mmol) and refluxed overnight. The cooling down to room temperature caused white powder precipitation. The solid was filtered, washed with hexane and subsequently H_2O (10 mL aliquots x 3 times). The obtained powder was dried under vacuum.

Yield: 53%. ATR-FTIR (ν, cm^{-1}): 3056 (aromatic CH stretch), 2955 (aliphatic CH stretch), 2867 (aliphatic CH stretch), 1995 (Ru-H), 1924 (C≡O), 1521 (asym. COO), 1480 (C=C-C), 1458 (sym. COO), 1432 (CH, PPh_3), (PPh), 1095 (PPh). ^{1}H NMR (400 MHz, $CDCl_3$) (δ, ppm): 7.45-7.30 (30 H, PPh_3, m), 6.69 (2 H, CH, d), 6.40 (2 H, CH, d), 2.41 (1 H, CH, q), 2.32 (2 H, CH_2, d), 1.75 (1 H, CH, dt), 0.84 (6 H, CH_3, dd), 0.53 (3 H, CH_3, d), -16.44 (1 H, Ru-H, t). ^{13}C NMR (101 MHz, $CDCl_3$) (δ, ppm): 205.59 (C≡O), 186.05 (COO), 139.00 (C), 138.92 (C), 134.44 (PPh_3), 133.91 (PPh_3), 129.79 (PPh_3), 128.64 (CH), 128.18 (PPh_3), 127.56 (CH), 47.61 (CH), 45.23 (CH_2), 30.31 (CH), 22.61 (CH_3), 17.90 (CH_3). ^{31}P NMR (162 MHz, $CDCl_3$) (δ, ppm): 43.30 (2P, PPh_3). ESI-MS$^+$ (MeCN) (m/z): 859 $[M-H]^+$.

3.7. X-Ray Crystallography

The X-ray intensity data for **4** and **5** were collected on a Bruker APEX CCD diffractometer using Mo–Kα or Cu-Kα radiation (for **5**). All data were processed using the Bruker suite of programs [35–37] and the structures were solved with SHELXT [38] and refined with the SHELXL programs [39]. All non-hydrogen atoms were assigned anisotropic displacement parameters. Most of the hydrogen atoms were located in the Fourier map, placed in idealized positions and included as riding with constrained isotropic displacement parameters for the aromatic and methyl protons and refined as riding with Uiso(H) = 1.2Ueq(C) or Uiso(H) = 1.3Ueq(C)methyl). Molecular graphics were generated

 doi:10.20944/preprints202601.1312.v1

using the program Mercury [40]. Table S1 reports crystal data and refinement parameters for **4** and **5**.

3.8. MTT Assay

Cells were seeded at 1.5×10^4 cells/well in a 96-well culture plastic plate (Sarsted, Milan, Italy), and after 24 h of growth were exposed to increasing concentrations of each distinct compound (from 1 μM to 100 μM) solubilized in RPMI 1640 medium. Controls were included and cells were either treated with DMSO.

MTT assay was performed according to the literature [41]. The absorbance at 570 nm was measured using a multiwell plate reader (Tecan, Männemorf, Switzerland), and data were analyzed by Prism GraphPad software. Percent cell viability was determined respect to control. All concentrations were tested in triplicates, and the experiment was repeated three times.

4. Conclusions

Metal coordination aims to combine anti-inflammatory effects with anticancer activities of the Ru-species, potentially leading to synergistic therapeutic novel effects. The synthesized compounds offer the simultaneous occurrence of carboxylic frames of NSAID's and phosphine ligands, therefore imparting amphiphilic features to Ru-core to be resilient in transferring to cancer targets. Herein we report ruthenium complexes coordinating four Non-Steroidal Anti-Inflammatory Drugs (NSAIDs), and the salicylate moiety as aspirin precursor, which have been synthesized, spectroscopically and structurally investigated. The rationale of the syntheses to novel Ru–NSAID complexes consists in providing pharmacophore molecules for targeting cancer, while ruthenium central core might provide further cytotoxic features, as DNA binding to trigger apoptosis via ROS mediation [16,19,33].

MTT assay on HeLa cancer cells performed by salicylic-complex **2** suggests antiproliferative activity, albeit in relatively elevated doses. Future perspectives include extending investigations to additional biological targets, such as interaction measures with Human Serum Albumin, Calf-Thymus DNA and Iron-carrier protein Transferrin. In summary, we believed that Ru-coordination should be responsible to promote synergistic effects by integrating complementary advantages, leading to improved tumor targeting and therapeutic outcomes by minimizing systemic toxicity, analogously to the findings in the case of small molecule-drug conjugates [42–44].

To pursuing the vision summarized in reducing pharmacological resistance and toxic effects, the attitudes of novel therapeutics emerge in enhancing benign impacts by penetrating exclusively cancer cells meanwhile exhibiting steady and durable efficacy with minimal administrated doses. However, many issues have to be overcome yet to allow the Ru-species to be tested as therapeutics in next clinical phases. Aiming at the ambitious health target, it would be auspicial for instance to improve both hydrolysis and metabolic absorption features of next-synthesized Ru-species [27].

Supplementary Materials: The following supporting information can be downloaded at the website of this paper posted on Preprints.org, Characterization of complexes: Figures S1-7, S9-40; Stability assessment of **2** through UV spectroscopy: Figure S8; X-ray diffraction studies: Table S1, Figures S41, S42.

Author Contributions: Conceptualization, S.B.; data curation, M.M., G.D. and F.M.; formal analysis, M.M.; funding acquisition, S.B.; investigation, G.D. and M.M.; methodology, S.B., G.D. and C.B.; project administration, S.B.; resources, S.B., M.M., and C.B.; supervision, S.B.; validation, S.B. and C.B.; writing—original draft, S.B., G.D. and F.M.; writing—review and editing, S.B., M.M., F.M. All authors have read and agreed to the published version of the manuscript.

Funding: This research was funded by Alma Mater Studiorum-Università di Bologna grant RFO 23 (to S.B.).

Institutional Review Board Statement: Not applicable.

Informed Consent Statement: Not applicable.

Data Availability Statement: The original contributions presented in the study are included in the article/supplementary material, further inquiries can be directed to the corresponding author/s.

Acknowledgments: We are deeply grateful to Natalia Calonghi for offering her expertise and teaching G.D. to discuss biological MTT assays. Her dedication and meticulous attention to detail significantly contributed to the quality and success of this research.

Conflicts of Interest: The authors declare no conflicts of interest.

References

1. Han Ang, W.; Dyson, P. J. Classical and Non-Classical Ruthenium-Based Anticancer Drugs: Towards Targeted Chemotherapy. *European Journal of Inorganic Chemistry* **2006**, *2006* (20), 4003–4018. https://doi.org/10.1002/ejic.200600723.
2. Bratsos, I.; Jedner, S.; Gianferrara, T.; Alessio, E. Ruthenium Anticancer Compounds: Challenges and Expectations. *Chimia* **2007**, *61* (11), 692. https://doi.org/10.2533/chimia.2007.692.
3. Kavukcu, S. B.; Özverel, C. S.; Kıyak, N.; Vatansever, H. S.; Türkmen, H. Ruthenium Compounds: Are They the next-Era Anticancer Agents? *Applied Organometallic Chemistry* **2024**, *38* (3), e7363. https://doi.org/10.1002/aoc.7363.
4. Lee, S. Y.; Kim, C. Y.; Nam, T.-G. Ruthenium Complexes as Anticancer Agents: A Brief History and Perspectives. *DDDT* **2020**, *14*, 5375–5392. https://doi.org/10.2147/DDDT.S275007.
5. Coverdale, J. P. C.; Laroiya-McCarron, T.; Romero-Canelón, I. Designing Ruthenium Anticancer Drugs: What Have We Learnt from the Key Drug Candidates? *Inorganics* **2019**, *7* (3), 31. https://doi.org/10.3390/inorganics7030031.
6. Zeng, L.; Gupta, P.; Chen, Y.; Wang, E.; Ji, L.; Chao, H.; Chen, Z.-S. The Development of Anticancer Ruthenium(II) Complexes: From Single Molecule Compounds to Nanomaterials. *Chem Soc Rev* **2017**, *46* (19), 5771–5804. https://doi.org/10.1039/c7cs00195a.
7. Tang, X.; Liang, X. Metal-Mediated Targeting in the Body. *Chemical Biology & Drug Design* **2013**, *81* (3), 311–322. https://doi.org/10.1111/cbdd.12090.
8. Ali, N. W.; Gamal, M.; Abdelkawy, M. Simultaneous Determination of Hyoscine N-Butyl Bromide and Paracetamol in Their Binary Mixture by RP-HPLC Method. *Arabian Journal of Chemistry* **2017**, *10*, S1868–S1874. https://doi.org/10.1016/j.arabjc.2013.07.015.
9. Starek, M.; Krzek, J. A Review of Analytical Techniques for Determination of Oxicams, Nimesulide and Nabumetone. *Talanta* **2009**, *77* (3), 925–942. https://doi.org/10.1016/j.talanta.2008.09.022.
10. Banti, C. N.; Hadjikakou, S. K. Non-Steroidal Anti-Inflammatory Drugs (NSAIDs) in Metal Complexes and Their Effect at the Cellular Level. *European Journal of Inorganic Chemistry* **2016**, *2016* (19), 3048–3071. https://doi.org/10.1002/ejic.201501480.
11. Cuzick, J.; Otto, F.; Baron, J. A.; Brown, P. H.; Burn, J.; Greenwald, P.; Jankowski, J.; Vecchia, C. L.; Meyskens, F.; Senn, H. J.; Thun, M. Aspirin and Non-Steroidal Anti-Inflammatory Drugs for Cancer Prevention: An International Consensus Statement. *The Lancet Oncology* **2009**, *10* (5), 501–507. https://doi.org/10.1016/S1470-2045(09)70035-X.
12. Czapski, G. A.; Czubowicz, K.; Strosznajder, J. B.; Strosznajder, R. P. The Lipoxygenases: Their Regulation and Implication in Alzheimer's Disease. *Neurochem Res* **2016**, *41* (1), 243–257. https://doi.org/10.1007/s11064-015-1776-x.
13. Kostova, I. Rational Design of Metal-Based Pharmacologically Active Compounds. *Inorganics* **2024**, *12* (12), 335. https://doi.org/10.3390/inorganics12120335.
14. Lucaciu Stan, R.; Hangan, A.; Sevastre, B.; Oprean, L. Metallo-Drugs in Cancer Therapy: Past, Present and Future. *Molecules* **2022**, *27*, 6485. https://doi.org/10.3390/molecules27196485.
15. Martling, A.; Hed Myrberg, I.; Nilbert, M.; Grönberg, H.; Granath, F.; Eklund, M.; Öresland, T.; Iversen, L. H.; Haapamäki, C.; Janson, M.; Westberg, K.; Segelman, J.; Ersson, U.; Prytz, M.; Angenete, E.; Bergström, R.; Mayrhofer, M.; Glimelius, B.; Lindberg, J. Low-Dose Aspirin for PI3K-Altered Localized Colorectal Cancer. *N Engl J Med* **2025**, *393* (11), 1051–1064. https://doi.org/10.1056/NEJMoa2504650.

 doi:10.20944/preprints202601.1312.v1

16. Oliveira, K. M.; Honorato, J.; Gonçalves, G. R.; Cominetti, M. R.; Batista, A. A.; Correa, R. S. Ru(II)/Diclofenac-Based Complexes: DNA, BSA Interaction and Their Anticancer Evaluation against Lung and Breast Tumor Cells. *Dalton Trans.* **2020**, *49* (36), 12643–12652. https://doi.org/10.1039/D0DT01591A.
17. Aman, F.; Hanif, M.; Siddiqui, W. A.; Ashraf, A.; Filak, L. K.; Reynisson, J.; Söhnel, T.; Jamieson, S. M. F.; Hartinger, C. G. Anticancer Ruthenium(η^6 - *p* -Cymene) Complexes of Nonsteroidal Anti-Inflammatory Drug Derivatives. *Organometallics* **2014**, *33* (19), 5546–5553. https://doi.org/10.1021/om500825h.
18. Ahmad Khan, R.; Al-Lohedan, H. A.; Abul Farah, M.; Sajid Ali, M.; Alsalme, A.; Mashay Al-Anazi, K.; Tabassum, S. Evaluation of (η^6 - *p*- Cymene) Ruthenium Diclofenac Complex as Anticancer Chemotherapeutic Agent: Interaction with Biomolecules, Cytotoxicity Assays. *Journal of Biomolecular Structure and Dynamics* **2019**, *37* (15), 3905–3913. https://doi.org/10.1080/07391102.2018.1528180.
19. Srivastava, P.; Mishra, R.; Verma, M.; Sivakumar, S.; Patra, A. K. Cytotoxic Ruthenium(II) Polypyridyl Complexes with Naproxen as NSAID: Synthesis, Biological Interactions and Antioxidant Activity. *Polyhedron* **2019**, *172*, 132–140. https://doi.org/10.1016/j.poly.2019.04.009.
20. Mandal, P.; Kundu, B. K.; Vyas, K.; Sabu, V.; Helen, A.; Dhankhar, S. S.; Nagaraja, C. M.; Bhattacherjee, D.; Bhabak, K. P.; Mukhopadhyay, S. Ruthenium(II) Arene NSAID Complexes: Inhibition of Cyclooxygenase and Antiproliferative Activity against Cancer Cell Lines. *Dalton Trans.* **2018**, *47* (2), 517–527. https://doi.org/10.1039/C7DT03637J.
21. Benadiba, M.; De M. Costa, I.; Santos, R. L. S. R.; Serachi, F. O.; De Oliveira Silva, D.; Colquhoun, A. Growth Inhibitory Effects of the Diruthenium-Ibuprofen Compound, [Ru2Cl(Ibp)4], in Human Glioma Cells in Vitro and in the Rat C6 Orthotopic Glioma in Vivo. *J Biol Inorg Chem* **2014**, *19* (6), 1025–1035. https://doi.org/10.1007/s00775-014-1143-4.
22. Sumithaa, C.; Ganeshpandian, M. Half-Sandwich Ruthenium Arene Complexes Bearing Clinically Approved Drugs as Ligands: The Importance of Metal–Drug Synergism in Metallodrug Design. *Mol. Pharmaceutics* **2023**, *20* (3), 1453–1479. https://doi.org/10.1021/acs.molpharmaceut.2c01027.
23. Golbaghi, G.; Castonguay, A. Rationally Designed Ruthenium Complexes for Breast Cancer Therapy. *Molecules* **2020**, *25* (2), 265. https://doi.org/10.3390/molecules25020265.
24. Graminha, A. E.; Popolin, C.; Honorato de Araujo-Neto, J.; Correa, R. S.; de Oliveira, K. M.; Godoy, L. R.; Vegas, L. C.; Ellena, J.; Batista, A. A.; Cominetti, M. R. New Ruthenium Complexes Containing Salicylic Acid and Derivatives Induce Triple-Negative Tumor Cell Death via the Intrinsic Apoptotic Pathway. *European Journal of Medicinal Chemistry* **2022**, *243*, 114772. https://doi.org/10.1016/j.ejmech.2022.114772.
25. Campideli, V. C.; Montilla-Suárez, J. M.; Silva, T. A.; Sicupira, D. C.; Oliveira, K. M.; Correa, R. S. Exploring DNA-Interaction and Molecular Structure of Ruthenium/1,2-Bis-(Diphenylphosphino)Ethane)-Based Complex. *European Journal of Chemistry* **2023**, *14* (2), 193–201. https://doi.org/10.5155/eurjchem.14.2.193-201.2402.
26. Teixeira, T.; Palmeira-Mello, M. V.; Machado, P. H.; Moraes, C. A. F.; Pinto, C.; Costa, R. C.; Badaró, W.; Gomes Neto, J. A.; Ellena, J.; Vieira Rocha, F.; Batista, A. A.; Correa, R. S. Ru(II)-Fenamic-Based Complexes as Promising Human Ovarian Antitumor Agents: DNA Interaction, Cellular Uptake, and Three-Dimensional Spheroid Models. *Inorg. Chem.* **2025**, *64* (8), 3707–3718. https://doi.org/10.1021/acs.inorgchem.4c04344.
27. Dong-Ling, K.; Ka-Kit, L.; Lai-Hon, C.; Jun, H.; Chun-Yuen, W. *Overview of Some Second- and Third-Row Late Transition Metal Pincer-Type N-Heterocyclic Carbene Complexes: Synthesis, Optical Properties, and Applications*. https://www.mdpi.com/1420-3049/30/12/2640 (accessed 2025-12-05).
28. Amaya-Flórez, A.; R.-Galindo, J.; Sanchez-Yocue, E.; Ruiz-Martinez, A.; Serrano-García, J. S.; Romo-Pérez, A.; Cano-Sanchez, P.; Reyes-Marquez, V.; Lagadec, R. L.; Morales-Morales, D. Cyclometalated Complexes: Promising Metallodrugs in the Battle against Cancer. *RSC Med. Chem.* **2025**, *16* (11), 5125–5195. https://doi.org/10.1039/D5MD00178A.
29. Tabrizi, L.; Olasunkanmi, L. O.; Fadare, O. A. Experimental and Theoretical Investigations of Cyclometalated Ruthenium(II) Complex Containing CCC-Pincer and Anti-Inflammatory Drugs as Ligands: Synthesis, Characterization, Inhibition of Cyclooxygenase and in Vitro Cytotoxicity Activities in Various Cancer Cell Lines. *Dalton Trans.* **2019**, *48* (2), 728–740. https://doi.org/10.1039/C8DT03266A.

 doi:10.20944/preprints202601.1312.v1

30. Correa, R. S.; De Oliveira, K. M.; Delolo, F. G.; Alvarez, A.; Mocelo, R.; Plutin, A. M.; Cominetti, M. R.; Castellano, E. E.; Batista, A. A. Ru(II)-Based Complexes with N-(Acyl)-N′,N′-(Disubstituted)Thiourea Ligands: Synthesis, Characterization, BSA- and DNA-Binding Studies of New Cytotoxic Agents against Lung and Prostate Tumour Cells. *Journal of Inorganic Biochemistry* **2015**, *150*, 63–71. https://doi.org/10.1016/j.jinorgbio.2015.04.008.
31. Hey, D. A.; Sauer, M. J.; Fischer, P. J.; Esslinger, E.-M. H. J.; Kühn, F. E.; Baratta, W. Acetate Acetylacetonate Ampy Ruthenium(II) Complexes as Efficient Catalysts for Ketone Transfer Hydrogenation. *ChemCatChem* **2020**, *12* (13), 3537–3544. https://doi.org/10.1002/cctc.202000542.
32. Pearson, R. G. Antisymbiosis and the Trans Effect. *Inorg. Chem.* **1973**, *12* (3), 712–713. https://doi.org/10.1021/ic50121a052.
33. Tadić, A.; Poljarević, J.; Krstić, M.; Kajzerberger, M.; Aranđelović, S.; Radulović, S.; Kakoulidou, C.; Papadopoulos, A. N.; Psomas, G.; Grgurić-Šipka, S. Ruthenium–Arene Complexes with NSAIDs: Synthesis, Characterization and Bioactivity. *New J. Chem.* **2018**, *42* (4), 3001–3019. https://doi.org/10.1039/C7NJ04416J.
34. Chen, J.; Zhang, Y.; Jie, X.; She, J.; Dongye, G.; Zhong, Y.; Deng, Y.; Wang, J.; Guo, B.; Chen, L. Ruthenium(II) Salicylate Complexes Inducing ROS-Mediated Apoptosis by Targeting Thioredoxin Reductase. *Journal of Inorganic Biochemistry* **2019**, *193*, 112–123. https://doi.org/10.1016/j.jinorgbio.2019.01.011.
35. APEX3 Software Package V2019; Bruker AXS Inc.: Madison, WI, **2019**.
36. Bruker SAINT, v8.40A: Part of the APEX3 Software Package V2019; Bruker AXS Inc.: Madison, WI, **2019.**
37. Bruker SADABS V2016/2: Part of the APEX3 Software Package V2019; Bruker AXS Inc.: Madison, WI, **2019**.
38. Sheldrick, G. SHELXT – Integrated Space-Group and Crystal-Structure Determination. *Acta Crystallographica Section A* **2015**, *71*, 3–8. https://doi.org/10.1107/S2053273314026370.
39. Sheldrick, G. M. Crystal Structure Refinement with SHELXL. *Acta Cryst C* **2015**, *71* (1), 3–8. https://doi.org/10.1107/S2053229614024218.
40. Macrae, C. F.; Sovago, I.; Cottrell, S. J.; Galek, P. T. A.; McCabe, P.; Pidcock, E.; Platings, M.; Shields, G. P.; Stevens, J. S.; Towler, M.; Wood, P. A. Mercury 4.0: From Visualization to Analysis, Design and Prediction. *J Appl Cryst* **2020**, *53* (1), 226–235. https://doi.org/10.1107/S1600576719014092.
41. Calonghi, N.; Farruggia, G.; Boga, C.; Micheletti, G.; Fini, E.; Romani, L.; Telese, D.; Faraci, E.; Bergamini, C.; Cerini, S.; Rizzardi, N. Root Extracts of Two Cultivars of Paeonia Species: Lipid Composition and Biological Effects on Different Cell Lines: Preliminary Results. *Molecules* **2021**, *26* (3), 655. https://doi.org/10.3390/molecules26030655.
42. Wang, X.; Guo, C.; Shao, J.; Zou, X.; Xing, S.; Xu, C. L.; Zhao, Q.; Wu, Y.; Sun, C.; Chen, Y.; Sun, H. Small Molecule-Drug Conjugates: An Emerging Drug Design Strategy for Targeted Therapeutics. *J. Med. Chem.* **2025**, *68* (23), 24759–24784. https://doi.org/10.1021/acs.jmedchem.5c01861.
43. Lerchen, H.-G.; Stelte-Ludwig, B.; Kopitz, C.; Heroult, M.; Zubov, D.; Willuda, J.; Schlange, T.; Kahnert, A.; Wong, H.; Izumi, R.; Hamdy, A. A Small Molecule–Drug Conjugate (SMDC) Consisting of a Modified Camptothecin Payload Linked to an αVß3 Binder for the Treatment of Multiple Cancer Types. *Cancers* **2022**, *14* (2), 391. https://doi.org/10.3390/cancers14020391.
44. Meng, F.; Qi, T.; Liu, X.; Wang, Y.; Yu, J.; Lu, Z.; Cai, X.; Li, A.; Duan, J. 20P The Essential Role of DNA Repair in the Pharmacological Activities of AST-3424. *Annals of Oncology* **2023**, *34*, S193. https://doi.org/10.1016/j.annonc.2023.09.1523.